

Evaluating singular and near-singular integrals on C^2 smooth surfaces with a novel geometric method and closed form expressions

Andrew Zheng¹, Spyros Alexakis¹, and Adam R. Stinchcombe¹

¹Department of Mathematics, University of Toronto, 40 St George Street, Toronto M5S 2E4, ON, Canada (andrewf.zheng@mail.utoronto.ca, alexakis@math.toronto.edu, stinch@math.toronto.edu).

February 2025

Abstract

Most Fredholm integral equations involve integrals with weakly singular kernels. Once the domain of integration is discretized into elements, these weakly singular kernels become strongly singular or “near-singular”. Common methods to compute these integrals when the kernel is a Green’s function include the Duffy transform, polar coordinates with closed analytic formulas, and singularity extraction. However, these methods do not generalize well to the normal derivatives of Green’s functions. We provide methods to integrate both the Green’s function and its normal derivative on smooth surfaces discretized by triangular elements in three dimensions. For strongly singular integrals involving normal derivatives of Green’s functions, we provide two methods that can accurately approximate the true integrals on the true domain. The Geometric method uses geometric information of the true surface of integration to approximate the original integral on the true domain using push-forward maps. The Interpolation-Duffy method heuristically cancels out the singularity and then evaluates the integral using a quadrature scheme. Both methods are better than simply setting the singular integrals to zero, while being faster than adaptive refinement methods. The explicit analytic formulas for integrating polynomials p of degree less than three are provided.

Contents

1	Introduction	2
2	Closed Form Equations for Near Singular Integrals	4
2.1	Choosing the correct polar coordinates	4
2.2	Determining start and end angles	5
2.3	Example	8
3	Two Novel Methods for Singular Integrals	8
3.1	Geometric Method	9
3.2	Calculating the Second Fundamental Form	11

3.3	Interpolation-Duffy Method	12
3.4	Comparison between the two methods	14
4	Results	14
4.1	Comparisons on near-singular integrals	14
4.2	Comparisons on singular integrals	14
5	Conclusion	17
6	Acknowledgments	20
7	Appendix	20
7.1	Formulas for near singular integrals	20
7.2	Formulas for the Geometric method	25
7.3	Formulas for Green's function	28

1 Introduction

Let $\Omega \subset \mathbb{R}^3$ with C^2 boundary. Consider the problem of integrating a function f over $\partial\Omega$. Assuming that $f \in L^1(\partial\Omega)$, this is a difficult problem numerically. Unless there are very easy analytic formulas that represent the integral, one will have to create a quadrature scheme for this integral. As the geometry of $\partial\Omega$ becomes more complicated, an accurate quadrature scheme will be harder and harder to find. One common algorithm to integrate functions on arbitrary smooth boundaries is to first discretize $\partial\Omega$ into elements on which very accurate quadrature schemes exist [10]. In 2D, common elements are line segments, while in 3D they are simplexes or triangles which we denote by Δ . The method of approximating $\partial\Omega$ with a finite number of triangles is often referred to as triangulation, and we denote by $\partial\Omega_\Delta$ as the collection of those triangles. There are many algorithms available that can perform this triangulation [16, 5] and simple implementations can be found in most commonly used programming languages.

Now that we have approximated $\partial\Omega$ with $\partial\Omega_\Delta$, we can write

$$I(f) = \int_{\partial\Omega} f(\underline{x}) dS(\underline{x}) \approx \sum_{\Delta \in \partial\Omega_\Delta} \int_{\Delta} f(\underline{x}) dS(\underline{x}). \quad (1.1)$$

However, the function f is usually weakly singular on $\partial\Omega$ and strongly singular on the triangles Δ . Thus, by triangulation, we approximate a finite integral with an undefined integral.

In the field of integral operators, partial differential equations (PDEs) are reformulated into integral equations. Some of these integral equations are Fredholm integrals of the form

$$u(\underline{x}) + \int_{\partial\Omega} K(\underline{x}, \underline{y}) u(\underline{y}) d\underline{y}. \quad (1.2)$$

The kernel function $K(\underline{x}, \cdot)$ is usually weakly singular on $\partial\Omega$. Through triangulation, the approximations of $\partial\Omega$ using elements creates new singularities in K that make it strongly singular.

A common example of a function that is weakly integrable on $\partial\Omega$ but not on its triangulation is the normal derivative of Green's function for the Laplace equation in three dimensions, which shows up in many electrostatics problems [9]. Letting

$$G_{\mathbb{R}^3}(\underline{x}, \underline{y}) = -\frac{1}{2\pi|\underline{x} - \underline{y}|}, \quad (1.3)$$

we have that its normal derivative in \underline{x} is

$$K_{\mathbb{R}^3}(\underline{x}, \underline{y}) = \frac{\partial G}{\partial n(\underline{x})}(\underline{x}, \underline{y}) = \frac{(\underline{x} - \underline{y}) \cdot n(\underline{x})}{4\pi |\underline{x} - \underline{y}|^3}. \quad (1.4)$$

In more generality, the integrals we want to evaluate are

$$\int_{\Delta} G(\underline{x}, \underline{y}) p(\underline{y}) dS(\underline{y}) = \int_{\Delta} \frac{g(\underline{x}, \underline{y})}{|\underline{x} - \underline{y}|} p(\underline{y}) dS(\underline{y}), \quad (1.5)$$

$$\int_{\Delta} \frac{\partial G}{\partial n(\underline{x})}(\underline{x}, \underline{y}) p(\underline{y}) dS(\underline{y}) = \int_{\Delta} \frac{f(\underline{x}, \underline{y}) \cdot n(\underline{x})}{|\underline{x} - \underline{y}|^3}(\underline{x}, \underline{y}) p(\underline{y}) dS(\underline{y}) \quad (1.6)$$

where G has a type $r^{-1} = |\underline{x} - \underline{y}|^{-1}$ singularity and f is a smooth function. Common examples that fit this frame work is the Green's function for 3D Laplace, Helmholtz, and Screened-Poisson equations. We also assume that p is some polynomial, and Δ is some triangle in \mathbb{R}^3 . This is because in most integral equations, one represents u in some basis of polynomials.

When evaluating Equation 1.5 when \underline{x} is very close to Δ , previous papers have presented methods involving the Duffy transform [7], polar coordinate systems [3], and singularity extraction methods [11]. Though they work well for integrals of the form Equation 1.5, they fail when trying to evaluate Equation 1.6. This is especially true when \underline{x} is in Δ . If one were to use the recursive formulas of [11] for Equation 1.6 with \underline{x} being a vertex of Δ , their answer would simply be zero if p is a constant. This is especially problematic as most polynomial basis functions include a constant term.

As \underline{x} approaches \underline{y} , the denominator behaves like r^3 . One power is canceled out from the $(\underline{x} - \underline{y})$ in the numerator, another is canceled out from $dS(\underline{y})$. When \underline{y} approaches \underline{x} , the dot product $(\underline{x} - \underline{y}) \cdot n(\underline{x})$ becomes orthogonal to $n(\underline{x})$. Thus, the original integrand on the C^2 boundary only has a removable singularity. On triangles, \underline{x} being very close to \underline{y} means that they are on the same triangle Δ . This results in $(\underline{x} - \underline{y})$ being on the same plane as the triangle for all $\underline{y} \in \Delta$. If Δ is not orthogonal to $n(\underline{x})$, a new singularity is introduced. If Δ is orthogonal to $n(\underline{x})$, then the entire integral is zero as the numerator is zero for all $\underline{y} \in \Delta$. Both cases result in very bad approximations of the true integral. Even if \underline{x} does not lie on Δ , just by being close enough, the integral can numerically appear singular, making the error large.

The fundamental problem of the integral Equation 1.6 when \underline{x} is in Δ is that we are trying to approximate the true weakly singular integral I_{true} with a strongly singular integral $I = \infty$. Previous analytic methods [11] then approximate this divergent integral by computing only its finite part. The Interpolation-Duffy (I-D) method approximates this divergent integral by computing an similar but augmented integral that is only weakly singular integral on a triangle. What both cases are trying to do is to approximate infinity with a finite value that hopefully is close to I_{true} . Instead of approximating an "infinity" that was intended to approximate I_{true} , we introduce a new evaluation method, which we call the geometric method, that directly approximates I_{true} by using geometric information of the true domain $\partial\Omega$.

The paper is divided into 3 parts. In section 2, we introduce analytical formulas that can integrate Equation 1.6 when \underline{x} is near Δ but not on it. In section 3, we present two different methods to handle the strongly singular integrals of Equation 1.6 when \underline{x} is a vertex of Δ . In section 4 we give numerical simulations of our new methods and see how they compare to the standard adaptive quadrature method of MATLAB. Finally, we end the paper with an appendix that gives explicit formulas of some integrals that arise in our methods for low degrees of p .

An implementation of our new methods in Rust is available on Github, and instructions on how to call it using C or Matlab are provided in the repository.

Through this paper, we use the notation that underlined variables \underline{x} represents vectors, while x represents a real value. We will use Δ to represent triangles instead of the Laplacian operator.

2 Closed Form Equations for Near Singular Integrals

We present a novel method to analytically evaluate our integrals on triangles that works for all cases except for when the target point \underline{x} lies inside the triangle Δ when integrating $K(\underline{x}, y)p(y)$. This is done by using a polar coordinate transform that greatly simplifies the integrand. Once in the new polar coordinate system, we give an algorithm that finds the bounds on integration that then gives explicit closed form formulas for the integral.

As \underline{x} becomes closer to Δ , the numerical integral starts to blow up, making it “near-singular”. Adaptive refinement of the triangles can give very accurate results in the near-singular case [1], but also greatly increases algorithm runtime.

Other papers have also tried to give analytic formulas, but either their formulas require special assumptions or need to split the triangle into special sub-triangles [4, 15, 2]. [8] gives very similar polar transforms as we do for near singular integrals, but we argue that our new algorithm for determining bounds on integration allows for more generalization. We consider the general case of evaluating Equation 1.6 on any arbitrary triangle Δ .

2.1 Choosing the correct polar coordinates

To obtain an analytic solution to our integral on a triangle, we use polar coordinates and a transformation that allows us to invoke Pythagoras’ theorem. Our transformations needs to preserve Euclidean distance, so it can only be a combinations of rotations and translations. We map Δ to a triangle Δ_{XY} that lies on the XY -plane, such that the point \underline{x} we are integrating it against lies on the Z -axis. This map is the rotational map between the triangle normal and the vector $[0, 0, 1]$, followed by a translation. Let $n(\Delta)$ be the normal vector of the arbitrary triangle. We want to find a map that rotates $n(\Delta)$ into $[0, 0, 1]^T$, the normal vector of a triangle that lies on the XY -plane. This rotational map R is the 3×3 matrix defined by

$$R = \cos(\alpha)I + (1 - \cos(\alpha)) * s^T s + \sin(\alpha) * [v]_{\times} \quad (2.1)$$

where we define

$$v = n(\Delta) \times \begin{bmatrix} 0 \\ 0 \\ 1 \end{bmatrix}, \quad \alpha = \arccos \left(n(\Delta) \cdot \begin{bmatrix} 0 \\ 0 \\ 1 \end{bmatrix} \right), \quad s = \frac{v}{\|v\|}$$

and $[v]_{\times}$ is the skew symmetric matrix of $v = \begin{bmatrix} v_1 \\ v_2 \\ v_3 \end{bmatrix}$ defined by

$$[v]_{\times} = \begin{bmatrix} 0 & -v_3 & v_2 \\ v_3 & 0 & -v_1 \\ -v_2 & v_1 & 0 \end{bmatrix}. \quad (2.2)$$

This is commonly known as Rodrigues’ rotation formula. After applying the rotation, a translation is done to map the triangle onto the XY -plane and the point $R(\underline{x})$ onto the Z -axis.

As \underline{x} lies on the Z -axis, we can write $\underline{x} = [0, 0, c]^T$. Pythagoras' theorem then gives $|\underline{x} - \underline{y}|^2 = y_x^2 + y_y^2 + c^2$, so the desired integral is

$$I = \int_{\Delta_{XY}} \frac{-y_x n_x - y_y n_y + c n_z}{(y_x^2 + y_y^2 + c^2)^{3/2}} p(\underline{y}) dS_{\underline{y}}.$$

Assuming that the polynomial p has degree at most 1, we simply need to compute the integrals

$$\begin{aligned} I_0 &:= \int_{\Delta} \frac{1}{(y_x^2 + y_y^2 + c^2)^{3/2}} dS_{\underline{y}}, & I_x &:= \int_{\Delta} \frac{y_x}{(y_x^2 + y_y^2 + c^2)^{3/2}} dS_{\underline{y}}, \\ I_y &:= \int_{\Delta} \frac{y_y}{(y_x^2 + y_y^2 + c^2)^{3/2}} dS_{\underline{y}}, & I_{x^2} &:= \int_{\Delta} \frac{y_x^2}{(y_x^2 + y_y^2 + c^2)^{3/2}} dS_{\underline{y}}, \\ I_{y^2} &:= \int_{\Delta} \frac{y_y^2}{(y_x^2 + y_y^2 + c^2)^{3/2}} dS_{\underline{y}}, & I_{xy} &:= \int_{\Delta} \frac{y_x y_y}{(y_x^2 + y_y^2 + c^2)^{3/2}} dS_{\underline{y}}. \end{aligned}$$

For example, if we consider $p(\underline{y}) = 1$, then the desired integral is

$$I = c n_z I_0 - n_x I_x - n_y I_y$$

Introducing polar coordinates for \underline{y} : $y_x = r \cos \theta$, $y_y = r \sin \theta$, we can rewrite the integrals into the form

$$\int_{r_{\text{start}}}^{r_{\text{end}}} \int_{\theta_{\text{start}}(r)}^{\theta_{\text{end}}(r)} \frac{r^{a+b+1} (\cos(\theta))^a (\sin(\theta))^b}{(r^2 + c^2)^{3/2}} d\theta dr$$

for powers (a, b) that represents the powers of y_x and y_y in the numerator. The method to determine the values of $\theta_{\text{start}}(r)$ and $\theta_{\text{end}}(r)$ are explained in the following subsection.

2.2 Determining start and end angles

When we integrate in polar coordinates starting at the point \underline{y} where the circle of radius r intersects an edge of the triangle, the angle $\theta(r)$ of the point \underline{y} can be written as

$$\theta_{\text{start}}(r) = \arccos\left(\frac{y_x}{r}\right) \quad (2.3)$$

However, y_x is non-linearly dependent on r , so this does not give rise to a simple analytic solution. Instead, we look at the projection of the origin to the lines which define the sides of the triangle. Let us label the positively oriented vertices as V_1, V_2, V_3 . Let d_1 be the projection of the origin to the line on which V_1 and V_2 lie on; d_2 be the projection of the origin to the line on which V_2 and V_3 lie on; and d_3 be the projection of the origin to the line on which V_3 and V_1 lie on.

Let ϕ_k be the angle between d_k and the X -axis, then the angle at a point of intersection between a circle of radius r and a side of the triangle is

$$\theta(r) = \pm \arccos\left(\frac{d_k}{r}\right) + \phi_k \quad (2.4)$$

where d_k is the orthogonal projection of the origin onto the line on which that specific edge of the triangle lies on. An example is shown in Figure 1. The importance of this equation is that now

$$\theta_{\text{start}}(r) = \text{sign}_{\text{start}} \arccos\left(\frac{d_{\text{start}}}{r}\right) + \phi_{\text{start}}$$

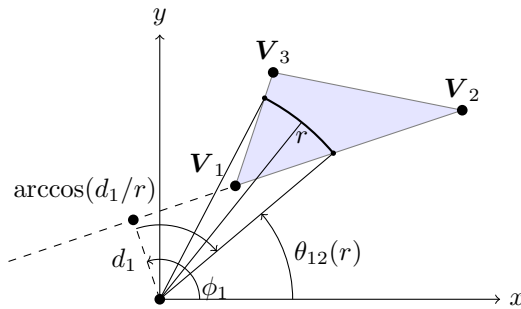


Figure 1: A diagram defining variables for the integration. The triangle Δ is defined by the points V_1, V_2, V_3 . The distance from the origin to the projection of the origin onto the side $\overline{V_1V_2}$ is d_1 ; this projection makes an angle of ϕ_1 with the X -axis. A circle of radius r centered at the origin intersects the side $\overline{V_1V_2}$ with an angle of $\theta_{12}(r)$ with the X -axis. Similarly, this circle intersects side $\overline{V_3V_1}$ with an angle of $\theta_{31}(r)$ with the X -axis.

where $\text{sign}_{\text{start}}, d_{\text{start}}, \phi_{\text{start}}$ are all piece-wise constant in r . If we split our integral into the correct regions in r , it is much simpler to write out an analytic solution to our integral.

The critical radii R_i which separates the regions on which $\text{sign}_{\text{start}}, d_{\text{start}}, \phi_{\text{start}}$ (and the corresponding end values) are constant are the norm of the three vertices of the triangle and the norm of the orthogonal projections d_k if they lie on the triangle, ordered from smallest to largest. Starting at $r = 0$, the θ integral is either on $[0, 2\pi]$ or on \emptyset , depending on if the origin is in the triangle. This is easily checked numerically. Now as we progress through the different critical radii, we need to keep track on which angles we start and stop the integration. This is done by labeling the triangle edges and keeping track of their activity.

Definition 2.1. For a given radius r , the edge $\overline{V_1V_2}$ of a triangle with vertices V_1, V_2, V_3 lying on the XY -plane is **inactive** if the circle of radius r on the XY plane does not intersect $\overline{V_1V_2}$. It is **active** if the circle of radius r intersects it only once, and **split** if it intersects it twice.

The reason for this definition is to know what angles we use in our integrals. For example, at $r = 0$, all edges are inactive unless the origin is one of the vertices, in which case two edges are active and one is inactive. If two edges are active while the third is inactive, then we only need to consider two angles and which one of them is the start angle and which is the end angle.

To make sure that we are always integrating in the correct direction, we need to first order the vertices of the triangle such that its vertices V_1, V_2, V_3 are positively oriented and V_1 is the vertex closest to the origin.

Definition 2.2. For a triangle in the previously specified configuration, if the projection point d_1 lies on the interior of the edge $\overline{V_1V_2}$, it splits the edge into $\overline{V_1d_1}$ and $\overline{d_1V_2}$, which we define as its **left** and **right** respectively. For other projection points, the left and right are defined so that everything is still positively oriented. If the projection point does not lie on the edge, that entire edge is considered as both left and right for the sake of the algorithm.

Note that when a projection point lies on an edge of the triangle, its left and right corresponds to different signs for arc-cosine. It is not trivial to determine which has the positive sign and which has the negative sign, so it must be computed by testing which sign of arc-cosine the vertices of that edge

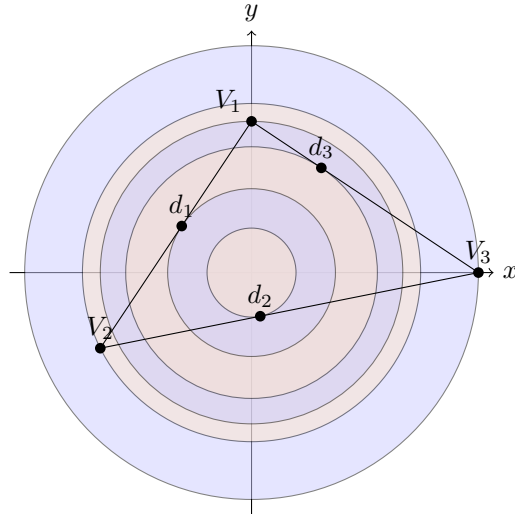


Figure 2: A diagram showing the different critical radii for integration. The triangle Δ is defined by the points V_1, V_2, V_3 . The projection of the origin to the edges of the triangles are labeled with d_1, d_2, d_3 , which in this case all lie on their respective edges. Letting -1 represent inactive, 1 represent active, and 0 represent split, the activities of the edges ordered in $[\overline{V_1V_2}, \overline{V_2V_3}, \overline{V_3V_1}]$ change as follows. Starting from $r = 0$, $[-1, -1, -1] \rightarrow [-1, 0, -1] \rightarrow [0, 0, -1] \rightarrow [0, 0, 0] \rightarrow [1, 0, 1] \rightarrow [-1, 1, 1] \rightarrow [-1, -1, -1]$

use. If d_1 lies on $\overline{V_1V_2}$, the simplest way is to check if which sign makes $V_1 = \pm \arccos\left(\frac{d_1}{\|V_1\|}\right) + \phi_1$ true. This configuration makes it so that we always integrate from edges $\overline{V_1V_2}$ to $\overline{V_2V_3}$ to $\overline{V_3V_1}$. In the case where an edge is split, we use Definition 2.2 to know that we always integrate starting the the right side of the first active or split edge and then alternate between left and right of the following edges.

As the radius r increases, the activity of the edges change when r equals to a critical radii. At $r = R_i$, the change in the activities is dependent on whether R_i is the norm of a vertex or a projection point. If it is the norm of a vertex, the activities of the edges the vertex lie on changes. Inactive edges become active while active edges become inactive. A split edge on the other hand becomes active. There is a special case where two vertices have the exact same norm, which can cause a split edge to become inactive. However, due to floating point precision, we do not consider this case. If R_i is the norm of a projection point, the only case that happens is the inactive edge that it lies on becomes split. An example of how the activities change is shown in Figure 2. For more details, check the comments in the code, which we outline other special cases.

This algorithm can then be used to integrate any function on any triangle that lies on \mathbb{R}^2 without the need to apply some non-distance preserving transform.

2.3 Example

Now that we can accurately determine the activity of each edge and which sign each arc-cosine has, we can integrate on the triangle. We denote

$$\begin{aligned}\theta_{\text{end}}(r) &= \text{sign}_{\text{end}} \arccos\left(\frac{d_{\text{end}}}{r}\right) + \phi_{\text{end}}, \\ \theta_{\text{start}}(r) &= \text{sign}_{\text{start}} \arccos\left(\frac{d_{\text{start}}}{r}\right) + \phi_{\text{start}}.\end{aligned}$$

The analytic formula for I_0 is

$$\begin{aligned}I_0 &= \int_{r_{\text{start}}}^{r_{\text{end}}} \int_{\phi_{\text{start}} + \text{sign}_{\text{start}} \arccos(d_{\text{start}}/r)}^{\phi_{\text{end}} + \text{sign}_{\text{end}} \arccos(d_{\text{end}}/r)} \frac{r}{(r^2 + c^2)^{3/2}} d\theta dr \\ &= (\phi_{\text{start}} - \phi_{\text{end}}) \int_{r_{\text{start}}}^{r_{\text{end}}} \frac{r}{(r^2 + c^2)^{3/2}} dr + \text{sign}_{\text{end}} \int_{r_{\text{start}}}^{r_{\text{end}}} \frac{r}{(r^2 + c^2)^{3/2}} \arccos\left(\frac{d_{\text{end}}}{r}\right) dr \\ &\quad - \text{sign}_{\text{start}} \int_{r_{\text{start}}}^{r_{\text{end}}} \frac{r}{(r^2 + c^2)^{3/2}} \arccos\left(\frac{d_{\text{start}}}{r}\right) dr\end{aligned}$$

The three integrals in r have analytic formulas which are found in Appendix 7.1. Other types of integrals once written in a similar form can also be evaluated by analytically evaluating the integrals in r by hand or by using mathematical programs like Mathematica.

Similar formulas are also obtained if we want to integrate Equation 1.5, and in this case the formulas also work for any arbitrary \underline{x} .

3 Two Novel Methods for Singular Integrals

In the previous section, we were able to directly integrate Equation 1.6 when $\underline{x} \notin \Delta$ because K was not singular on Δ . Once $x \in \Delta$, the integral becomes strongly singular and all the previous formulas fail. Specifically, some of the integrals in r become divergent. As the pre-discretization integral are clearly not infinite, we stress that this is due to the process of approximating a C^2 boundary with flat triangles, and not a feature of the integral we are trying to approximate.

Let V_1, V_2, V_3 be three points on the surface $\partial\Omega$ and let $\partial\Omega_V \subset \partial\Omega$ be the curved triangular patch on which we want to integrate our function. The specifics of how to define this triangular patch is discussed later. The true integral we want to evaluate is

$$I_{\text{true}} = \int_{\partial\Omega_V} \frac{\partial G}{\partial n(\underline{x})}(\underline{x}, \underline{y}) p(\underline{y}) dS(\underline{y}). \quad (3.1)$$

In this section, we give two different methods to approximate I_{true} when \underline{x} is one of the vertices of the triangular patch. Without loss of generality, let us assume that $\underline{x} = V_1$. This commonly occurs in numerical algorithms [10] as the points \underline{x} are usually collocation points chosen to be vertices of the triangles in $\partial\Omega_\Delta$.

As stated before, if we approximate $\partial\Omega_V$ with a flat triangle Δ , this integral becomes undefined. Thus, we need to either keep the true domain of integration, or we integrate a new function on Δ whose integral value is finite and hopefully approximates I_{true} . Previous methods that keep the true domain $\partial\Omega_V$ do not have explicit generalizable formulas [13], or are applicable only in the 2D setting with line elements [19]. Others use the second approach and simply integrate the zero function on

Δ , or only evaluate the finite part of the divergent integral [11]. The second approach can be viewed as trying to approximate infinity with a finite value that hopefully is close to I_{true} .

We first present the Geometric method, which keeps the domain to be $\partial\Omega_V$ and approximates it with analytic closed form expressions. We then present the I-D method, which approximates the domain with Δ , but integrates a heuristically chosen similar integral that is a weakly singular integral.

3.1 Geometric Method

Instead of approximating an “infinity” that was intended to approximate I_{true} , the Geometric method directly approximates I_{true} by using geometric properties of the true domain $\partial\Omega$.

Let us first rotate and shift the coordinate system so that V_1 is the origin and its normal vector $n(V_1) = (0, 0, 1)^T$. Using (s_1, s_2) as the coordinate system for the XY-plane that is now tangent to $\partial\Omega$, we have a push-forward map π_* from the (s_1, s_2) -plane onto a local region of $\partial\Omega$ that contains the three vertices. Let pV_2 and pV_3 be the projections of V_2 and V_3 onto the (s_1, s_2) -plane and $\Delta(pV_1pV_2pV_3)$ be the triangle that joins V_1, pV_2 , and pV_3 . Let $\partial\Omega_V$ denote the triangular patch on $\partial\Omega$ defined by $\pi^{-1}(\Delta(pV_1pV_2pV_3))$. With our rotations, the (s_1, s_2) -plane is tangent to $\partial\Omega_V$ and $\partial\Omega_V$ can be represented as a graph $s_3 = f(x^1, x^2)$.

Instead of approximating the integral on $\partial\Omega_V$ by integrating the same integrand on $\Delta(pV_1pV_2pV_3)$, we instead integrate directly on $\partial\Omega_V$ using a push-forward map. Integration on these curved triangular patches has been presented before [3], but only with singularity r^{-1} .

Let us denote the desired integral as

$$I = \int_{\partial\Omega_V} \frac{(V_1 - \underline{y}) \cdot n(V_1)}{|V_1 - \underline{y}|^3} p(\underline{y}) dS(\underline{y}). \quad (3.2)$$

Using the push-forward map, the integral can also be written as

$$I = \int_{p(V_1V_2V_3)} \pi_* \left[\frac{(V_1 - \underline{y}) \cdot n(V_1)}{|V_1 - \underline{y}|^3} p(\underline{y}) \right] \pi_* [dS(\underline{y})]. \quad (3.3)$$

As $V_1 = 0$, and $n(V_1) = (0, 0, 1)^T$, the integral simplifies to

$$I = \int_{p(V_1V_2V_3)} \pi_* \left[(-\underline{y}) \cdot \begin{bmatrix} 0 \\ 0 \\ 1 \end{bmatrix} |\underline{y}|^{-3} p(\underline{y}) \right] \pi_* [dS(\underline{y})]. \quad (3.4)$$

As we positioned our tangent plane to intersect the surface at the origin, $dS(\underline{y})$ and $\pi_*[dS(\underline{y})]$ differ by $O(|\underline{y}|^2)$ [20]. Since $\underline{y} \in \partial\Omega_V$ can be represented as $(s_1, s_2, f(s_1, s_2))$, we wish to approximate $f(s_1, s_2)$. The second fundamental form K_{ij} (expressed in the basis ∂_1, ∂_2 corresponding to (s_1, s_2)) of $\partial\Omega_j$ at V_1 is the Hessian of f at V_1 .

$$K_{ij}(V_1) = [\partial_{ij}f](V_1). \quad (3.5)$$

In the special case of Ω_j being a sphere of radius R , the second fundamental form is $K_{ij} = -R^{-1}\delta_{ij}$ where we use the outward pointing normal. Using the Taylor expansion of f at $V_1 = 0$, we have

$$\pi_* \left[\underline{y} \cdot \begin{bmatrix} 0 \\ 0 \\ 1 \end{bmatrix} \right] = \sum_{i,j=1}^2 \frac{1}{2} \partial_{ij}f(V_1) \cdot s_i s_j + O(|(s_1, s_2)|^3) = \sum_{i,j=1}^2 \frac{1}{2} K_{ij} s_i s_j + O(|(s_1, s_2)|^3). \quad (3.6)$$

This is because $f(0) = 0$ and all first order derivatives of f are zero as $\partial\Omega_V$ is tangent to the (s_1, s_2) -plane. We can also approximate $f(s_1, s_2)$ with only the first degree Taylor expansion with error $O(|(s_1, s_2)|^2)$, so $|y|^{-3} = (s_1^2 + s_2^2)^{-3/2} + O(|(s_1, s_2)|^2)$. Hence, our integral becomes

$$I = -\frac{1}{2} \int_{\Delta(pV_1pV_2pV_3)} \pi_*[p](s_1, s_2) \sum_{i,j=1}^2 K_{ij} s_i s_j [(s_1)^2 + (s_2)^2]^{-\frac{3}{2}} d(s_1, s_2) + O(|(s_1, s_2)|^2). \quad (3.7)$$

Now we wish to approximate $\pi_*[p]$ via a polynomial function. Using our previous interpolation method, we have that

$$\pi_*[p](x^1, x^2) \approx \sum_{k=1}^M \pi_*[p](pQ_k) l_k(x^1, x^2), \quad (3.8)$$

for some quadrature points $pQ_k \in \Delta(pV_1pV_2pV_3)$. Each pQ_k is the projection of a point $Q_k \in \partial\Omega_V$ onto the (x^1, x^2) -plane. By definition of the push-forward, we get that this is equivalent to

$$\pi_*[p](x^1, x^2) \approx \sum_{k=1}^M p(Q_k) l_k(x^1, x^2). \quad (3.9)$$

If we choose a quadrature with enough nodes, this is exact for our polynomial p , so there is no error in this part of the formula. Hence, our integral is approximately

$$I \approx \sum_{k=1}^M -\frac{p(Q_k)}{2} \int_{\Delta(pV_1pV_2pV_3)} \sum_{i,j=1}^2 K_{ij} x^i x^j l_k(x^1, x^2) [(x^1)^2 + (x^2)^2]^{-3/2} d(x^1) d(x^2) \quad (3.10)$$

and the error is approximately quadratic in $|y|$. Due to the lack of constant terms in the numerator, the integral always exists. Converting to polar coordinates, we have integrals of the form

$$\int_{\Delta(pV_1pV_2pV_3)} r^{a+b+1-3} (\cos(\theta))^a (\sin(\theta))^b d\theta dr, \quad (3.11)$$

where a and b non-negative integers that represent the powers of the two coordinates in the polynomials l_k .

Instead of integrating in θ first like before, we integrate in r first and then integrate in θ . The reason for this is due to the fact that pV_1 is the origin. Having a fixed vertex at the origin means that we can perform a rotation so that pV_2 lies on the positive s_1 -line, which then means that the integral in θ is a single segment unlike in previous cases. Let $\Delta(pV_1pV_2pV_3)$ be positively oriented and use a rotation such that pV_2 lies on the s_1 -axis. This way, $\theta \in [0, \theta_{pV_3}]$ where θ_{pV_3} is the angle of pV_3 and the s_1 -axis. As a function of θ , we have that

$$r(\theta) = \frac{|pV_2| \sin(\theta_2)}{\sin(\theta + \theta_2)}, \quad (3.12)$$

where θ_2 is the angle between pV_1pV_2 and pV_2pV_3 . This equation is obtained using the sine law, which states that

$$\frac{\sin(\theta_2)}{r} = \frac{\sin(\pi - \theta - \theta_2)}{|pV_2|}. \quad (3.13)$$

For a visualization, see Figure 3. Hence the integrals we need to compute are of the form

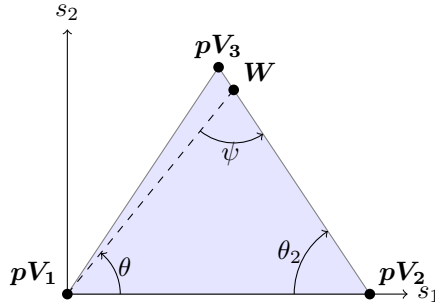


Figure 3: A diagram showing how to calculate $r(\theta)$. As θ grows, the sine law gives that the ratio between r and $\sin(\theta_2)$ is the same as the ratio between $|pV_2|$ and $\sin(\psi)$.

$$\int_0^{\theta_{\text{end}}} (\cos(\theta))^a (\sin(\theta))^b \int_0^{r(\theta)} r^{a+b+1-3} dr d\theta. \quad (3.14)$$

The integrals in r are trivial as $a + b + 1 - 3 \geq 0$, so we get

$$\int_0^{\theta_{\text{end}}} (\cos(\theta))^a (\sin(\theta))^b \frac{1}{a + b - 1} \left(\frac{|pV_2| \sin(\theta_2)}{\sin(\theta + \theta_2)} \right)^{a+b-1} d\theta. \quad (3.15)$$

Letting

$$\begin{aligned} \tilde{I}_{x^2} &= \int_0^{\theta_{\text{end}}} \frac{\cos^2(\theta)}{\sin(\theta + \theta_2)} d\theta, & \tilde{I}_{y^2} &= \int_0^{\theta_{\text{end}}} \frac{\sin^2(\theta)}{\sin(\theta + \theta_2)} d\theta, \\ \tilde{I}_{x^2y} &= \int_0^{\theta_{\text{end}}} \frac{\cos^2(\theta) \sin(\theta)}{\sin^2(\theta + \theta_2)} d\theta, & \tilde{I}_{xy^2} &= \int_0^{\theta_{\text{end}}} \frac{\cos(\theta) \sin^2(\theta)}{\sin^2(\theta + \theta_2)} d\theta, \\ \tilde{I}_{x^3} &= \int_0^{\theta_{\text{end}}} \frac{\cos^3(\theta)}{\sin^2(\theta + \theta_2)} d\theta, & \tilde{I}_{y^3} &= \int_0^{\theta_{\text{end}}} \frac{\sin^3(\theta)}{\sin^2(\theta + \theta_2)} d\theta, \end{aligned}$$

the desired integral can be written as some linear combination of these integrals. The formulas for $\tilde{I}_{x^2}, \dots, \tilde{I}_{y^3}$ can be found in Appendix subsection 7.2.

An important remark is that the Geometric method can still be used when \underline{x} is not a vertex. The only difference is that now we can no longer position the triangle to have one edge on the s_1 -axis. We would instead need to determine bounds of integration using the algorithm from the previous section 2.

3.2 Calculating the Second Fundamental Form

Since the Geometric method requires knowledge of the second fundamental form of a surface, we explain what it is and how to calculate it numerically. Intuitively, the second fundamental form is an extrinsic curvature that describes how curved a surface is. For a more rigorous and geometric understanding, see [20, 6] or any textbook on Differential Geometry. The theory contains many definitions and notions of fundamental forms, but we present a simple method of computing the second fundamental form for manifolds embedded in the standard Euclidean metric of \mathbb{R}^3 . Given

a point $\underline{y} \in \partial\Omega$, we first perform rotations and translations so that the surface is tangent to the XY -plane, intersects it at the origin, and the outward normal is pointing up. If the surface $\partial\Omega$ is the graph of a function $z = f(s_1, s_2)$, then the second fundamental form at the point (x, y) is $K_{ij} = \frac{\partial^2 f}{\partial s_i \partial s_j}(x, y)$. It is just the coefficients of the second order terms in the Taylor expansion of f at (x, y) .

For the sphere of radius R centered at the origin, we first apply a rotation so that $(x, y) = (0, 0)$ and that we are on the upper half of the sphere. Locally, we have that $z = \sqrt{R^2 - x^2 - y^2}$. Thus, its Taylor expansion is

$$z = R - \frac{1}{R}x^2 - \frac{1}{R}y^2 + \dots \quad (3.16)$$

Hence, $K_{ij} = -\delta_{ij}R^{-1}$ as we stated before.

This shows that if the user can locally represent the surface as the graph of a function, the second fundamental form can be explicitly calculated analytically. If the surface is defined only by a collection of points in a mesh and no such parametrization function is available, one can still approximate the second derivatives. At any point \underline{y} in the mesh, you can use a finite difference scheme and the nearby mesh points to approximate the second derivative [12].

3.3 Interpolation-Duffy Method

We now present the I-D method, which is a quadrature method inspired by the generalized Duffy transform [14]. Unlike the Geometric method, the I-D method does not use any geometric information of the boundary, thus it is much less accurate than the Geometric method. We introduce it only as a comparison and as another method that still does better than simply setting the integral to zero.

To simplify the integration, we first find the affine map T which maps the unit simplex Δ_S to Δ . Here, the unit simplex is defined as

$$\Delta_S = \{(s, t, 0) \in \mathbb{R}^3 : s + t = 1, 0 \leq s \leq 1, 0 \leq t \leq 1\}. \quad (3.17)$$

This exists as Δ is a flat triangle in \mathbb{R}^3 , so T is just a composition of rotations, shears, and translations. Furthermore, it is easy to see that the Jacobian of T is a constant which is just $J(T) = \frac{1}{2}\text{Area}(\Delta)$. Since \underline{x} is a vertex of Δ , we choose the map T that maps the origin to \underline{x} .

Now, we can write our integral as

$$J(T) \int_{\Delta_S} \frac{(\underline{x} - T(s, t)) \cdot \underline{n}(\underline{x})}{|\underline{x} - T(s, t)|^3} p(T(s, t)) dA. \quad (3.18)$$

As the singularity is at the origin, we can use the Duffy transform, which maps the unit square to the unit simplex via

$$s = (1 - s_2)s_1^\beta, \quad t = s_1^\beta s_2. \quad (3.19)$$

Choosing $\beta = 1$, this makes singularities of type r^{-1} removable, which one would think matches our kernel function. One of the powers in the denominator is canceled out by the $(\underline{x} - \underline{y})$ and another is canceled from the dot product between $(\underline{x} - \underline{y})$ and $\underline{n}(\underline{x})$, however the second statement is not true on Δ . Even when \underline{y} approaches \underline{x} , the dot product does not approach zero as \underline{y} is a point in Δ and not in $\partial\Omega$. Given a triangle Δ in our triangulation and a map $T : \Delta_S \rightarrow \Delta$, we have that the normal vector on Δ can be represented as

$$\underline{n}(\Delta) = \pm \frac{\frac{\partial T}{\partial s} \times \frac{\partial T}{\partial t}}{\left| \frac{\partial T}{\partial s} \times \frac{\partial T}{\partial t} \right|}. \quad (3.20)$$

It is the cross product of two sides of the triangle, and the sign is chosen so that it is the outward normal.

Some authors that encounter this strongly singular integral simply approximate it by setting it to zero [17, 18, 2], with the reasoning that they choose the normal $n(\underline{x})$ to just be $n(\Delta)$. As $(\underline{x} - \underline{y})$ lives on the same plane as Δ , $n(\underline{x}) \cdot (\underline{x} - \underline{y}) = 0$ so the strongly singular integral is set to be zero. Their reasoning is that with a fine enough triangulation mesh, the principle value integral is zero.

Instead of following the approach of these authors, we propose another idea that may solve this problem that does not require very fine meshes. To make sure that the dot product with the normal vector $n(\underline{x})$ still cancels out one of the singularities, we require that as \underline{y} approaches \underline{x} , $(\underline{x} - \underline{y})$ becomes orthogonal to $n(\underline{x})$. However, away from \underline{x} , we do not want $(\underline{x} - \underline{y}) \cdot n(\underline{x})$ to simply be zero, as that would defeat the purpose of even trying to evaluate the singular integral.

We define an augmented normal vector $N(\underline{x}, \underline{y})$ on a triangle Δ as a function similar to a convex combination of its true normal vector and the normal vector of the triangle Δ .

$$N(\underline{x}, \underline{y}) = \alpha n(\underline{x}) + (1 - \alpha)n(\Delta) \quad (3.21)$$

where α as defined as a rapidly changing smooth bump function:

$$\alpha(y) = \begin{cases} 0, & \text{if } \beta \leq a_1 \\ 1 - \exp\left(1 + \frac{1}{(a_3(\beta - a_1))^2 - 1}\right), & \text{if } a_1 < \beta \leq a_2 \\ 1, & \text{if } \beta > a_2 \end{cases} \quad (3.22)$$

and

$$a_3 = \frac{1}{a_2 - a_1}, \quad \beta = \frac{|\underline{x} - \underline{y}|}{\max_{\underline{y} \in \Delta} |\underline{x} - \underline{y}|}. \quad (3.23)$$

We choose $a_2 = a_1 + 0.1$ and

$$a_1 = \begin{cases} 0.40 - 0.37 \max_{\underline{y} \in \Delta} |\underline{x} - \underline{y}|, & \max_{\underline{y} \in \Delta} |\underline{x} - \underline{y}| > 0.1 \\ 0.418 - 0.55 \max_{\underline{y} \in \Delta} |\underline{x} - \underline{y}|, & \max_{\underline{y} \in \Delta} |\underline{x} - \underline{y}| \in (0.05, 0.1] \\ 0.4187 - 0.62 \max_{\underline{y} \in \Delta} |\underline{x} - \underline{y}|, & \max_{\underline{y} \in \Delta} |\underline{x} - \underline{y}| \in (0.01, 0.05] \\ 1.0, & \max_{\underline{y} \in \Delta} |\underline{x} - \underline{y}| \leq 0.01 \end{cases}.$$

These were chosen after multiple tests. The true optimal values we hypothesize should be some polynomial of degree at least two or a function that behaves like $f(x) = 1/x$ while depending on the curvature of the geometry and the edge lengths of the triangle. When \underline{y} becomes sufficiently close to \underline{x} , the augmented normal vector $N(\underline{x}, \underline{y})$ becomes perpendicular to $(\underline{x} - \underline{y})$, which makes the singularity removable. As \underline{y} gets further away from \underline{x} , $N(\underline{x}, \underline{y})$ rapidly becomes $n(\underline{x})$. Hence, this augmented kernel function has a singularity of type $\alpha = 1$ at the origin, so the Duffy transform makes it twice differentiable on the unit square. Hence, the convergence rate with increasing number of nodes on the unit square follows the theory for twice differentiable functions. A simple quadrature scheme for the unit square is the tensor product of Gauss-Legendre quadrature, though others can also be used.

As our choice of how to define $N(\underline{x}, \underline{y})$ can be viewed as a heuristic approximation, we believe that this I-D method is not the best method of approximating the true integral. It is simply a method that allows quadrature methods to approximate the true integral with a similar, but different, integral that does not diverge.

3.4 Comparison between the two methods

The Geometric method is much faster than the I-D method due to the I-D method potentially using a large number of quadrature nodes on the unit square. The Geometric method is also approximating the true integral on $\partial\Omega$, while the I-D method is evaluating an augmented finite integral on Δ that hopefully approximates the true finite integral on $\partial\Omega$. However, the Geometric method requires knowledge of the second fundamental form of $\partial\Omega$, which requires an extra step to compute.

4 Results

To test our new methods for calculating integrals, we test them based on their accuracy and time. For accuracy, we calculate the relative absolute difference of the values computed via the different methods and Matlab's `integral2` function. `integral2` uses adaptive quadrature, which is known to be accurate for small enough tolerance. For time, we record the wall-clock time of calculating each integral. For the I-D method, we use a 7×7 Gauss-Legendre quadrature rule on the unit square.

4.1 Comparisons on near-singular integrals

Let us consider evaluating the integral

$$I = \int_{\Delta} \frac{(\underline{x} - \underline{y}) \cdot n(\underline{x})}{4\pi|\underline{x} - \underline{y}|^3} dS(\underline{y}) \quad (4.1)$$

where Δ is a triangle in the triangulation approximation of the boundary $\partial\Omega = S^1$. We first present our results on the analytic equations given to evaluate the case when \underline{x} does not lie in Δ . As stated in previous sections, the integral is not singular at all, but its behaviour is near-singular. The integral is evaluated in 2000 different tests. In each test, the first two components of Δ 's vertices are uniformly sampled from $[-0.05, 0.05]$ while the third component is calculated so that the vertices lie on S^1 . $\underline{x} = [0, 0, c]$ where c is uniformly sampled from $[-0.05, 0.05]$ but its normal vector $n(\underline{x})$ is fixed to be $[\sqrt{3}/3, \sqrt{3}/3, \sqrt{3}/3]$. This is because after rotations, the normal vectors $n(\underline{x})$ are different in each test case. The results of these tests are shown in Figure 4. In terms of runtime, the analytic method is on average a thousand times faster than `integral2`, which uses an adaptive refinement algorithm. This difference in time can be reduced if the absolute and relative tolerances for `integral2` are increased. However, due to the different programming languages, the wall-times cannot be directly compared. Even when calculating

$$I = \int_{\Delta} \frac{(\underline{x} - \underline{y}) \cdot n(\underline{x})}{4\pi|\underline{x} - \underline{y}|^3} y_x dS(\underline{y}), \quad (4.2)$$

where y_x is the first component of \underline{y} , we obtain very similar results shown in Figure 5.

For integrals that do not have strong singularities at all, such as Equation 1.5, its similar analytic equations give the same accuracy. Though these equations give values that are very accurate, this analytic method is slower than a simple 3-point quadrature method due to the algorithm to find the bounds of integration. It is up to the users to decide when to use this analytic method and when to use a n -point quadrature method with small n .

4.2 Comparisons on singular integrals

In the next test, we still consider Equation 4.1 but now $\underline{x} = (0, 0, 0)$ is one of its vertices. In each test case, Δ is simulated the same way as the previous tests, but now \underline{x} and $n(\underline{x})$ are fixed so that \underline{x} is the

Relative Difference of Analytic Method compared to `integral2`
On Near Singular Kernel

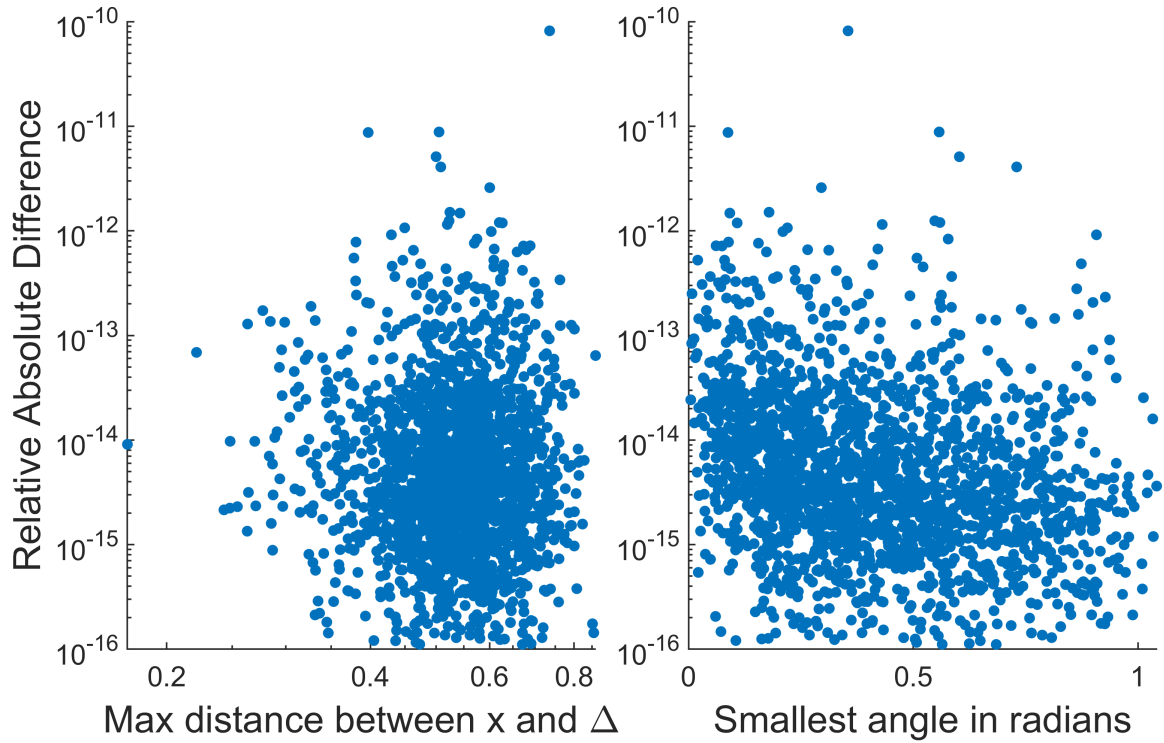


Figure 4: Comparison between the values of the integral Equation 4.1 using the Analytic Method and an adaptive method using `integral2` from Matlab on 2000 tests. Δ is assumed to have vertices on S^1 with their first two components uniformly distributed in $[-0.05, 0.05]^2$. $\underline{x} = [0, 0, c]$ where c is uniformly distributed in $[-0.05, 0.05]$. Absolute and relative tolerance for `integral2` was set to 10^{-14} . The relative difference between the two methods is always below 10^{-10} .

Relative Difference of Analytic Method compared to `integral2`
On Near Singular Kernel

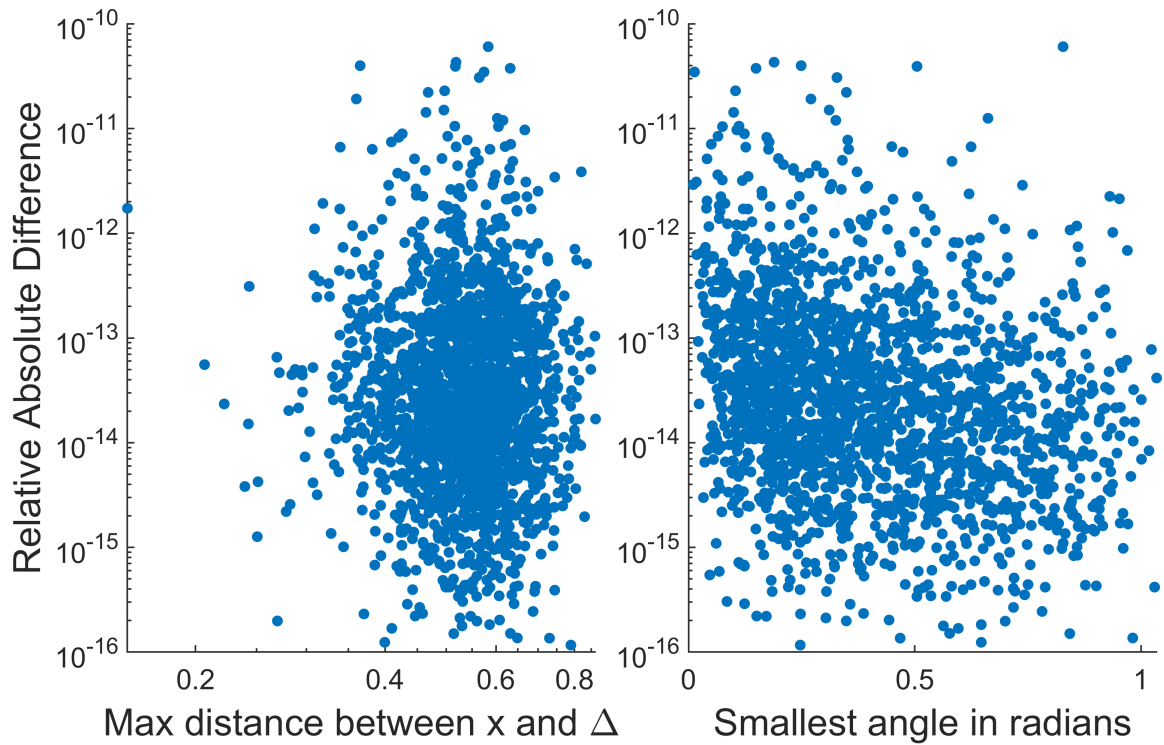


Figure 5: Comparison between the values of the integral Equation 4.2 using the Analytic Method and `integral2` on 2000 tests. Δ is assumed to be on the XY -plane with vertices uniformly distributed in $[-0.05, 0.05]^2$. $\underline{x} = [0, 0, c]$ where c is uniformly distributed in $[-0.05, 0.05]$. Absolute and relative tolerance for `integral2` was set to 10^{-14} . The relative difference between the two methods is always below 10^{-7} .

first vertex of Δ and its normal is the normal vector of S^1 at \underline{x} . When running the adaptive method, we actually integrate $K(\underline{x}, \underline{y})$ on the true triangular patch on S^1 . This is because the integral on Δ is divergent.

Since `integral2` is evaluating the true integral on a subset on S^1 , the relative difference of the I-D method compared to `integral2` is very high. This is because a lot of accuracy is lost the moment we approximate a smooth curved domain with piecewise linear planar triangles. In comparison, the Geometric method is much more accurate as it incorporates geometric properties of $\partial\Omega$ into its calculations to actually evaluate on $\partial\Omega$.

For the Geometric method, the closer the region of integration is to the origin, the better it approximates the adaptive method. Hence, larger triangles result in larger approximation errors. In the log-log plot, we see that the line that upper bounds the error has a slope of approximately two, which is what our analysis in section 3 stated.

For the I-D method, the relative difference in the I-D method compared to `integral2` seems to be more related to the shape of the triangles Δ and not its size. This is shown as the relative error seems to decrease in the right subplot of Figure 6. However, we believe that this error can be reduced if better methods of interpolating the normal vector (such as using some geometric information) are found. More accurate quadrature rules on the unit square can also be used to give better results. However, without information of $\partial\Omega$, we do not expect the I-D method to get as accurate as the Geometric method.

It is also important to note that if the tolerance is decreased, `integral2` will start to give warnings. Hence, it is not known if `integral2` is the best approximation of the true integral values. Unfortunately, analytic equations for the true solution are not available for this example on S^1 , so we can only compare to `integral2`. In terms of runtime, Figure 7 shows that the Geometric method is around ten times faster than the I-D methods. Though both methods look to be significantly faster than `integral2`, the times are not directly comparable as Matlab is not a compiled language. However, both methods are still likely to be much faster than adaptive methods as both methods require much less calculations.

5 Conclusion

In the fields of numerical PDEs, many problems are reformulated into integral equations. For Fredholm integral equations, the kernel functions are often weakly singular, and becomes strongly singular when the domain of integration is approximated by a finite number of elements. This is often the case in boundary element methods (BEM), so it is vital to be able to calculate these integrals accurately. Previous practices include setting the strongly singular integrals to zero and stating the error is bounded by the size of the simplex, evaluating only the non-singular part of the integral, or using adaptive refinement with a combination of the previous methods. Most previous analytic methods were only applicable to the 2D case, or when the singularity was of type $r^n, n \geq -1$.

However, with our new methods, we can provide fast computational algorithms that lowers the error of these strongly singular integrals even the case where the kernel function $K(\underline{x}, \underline{y})$ has singularity r^{-2} . The Interpolation-Duffy method uses a quadrature rule on the unit square and interpolates the normal vector $n(\underline{x})$ to heuristically stop the new domain Δ from introducing a new singularity. The Geometric method incorporates the true geometry of $\partial\Omega$ in a push-forward map so that the singularity caused by approximating $\partial\Omega$ by Δ is never present in the first place. Both methods are better than simply setting the integral to zero and much faster than adaptive refinement methods, but the Geometric method is much more accurate than the Interpolation-Duffy method as it integrates on the true geometry. However, the Geometric method requires an extra step of

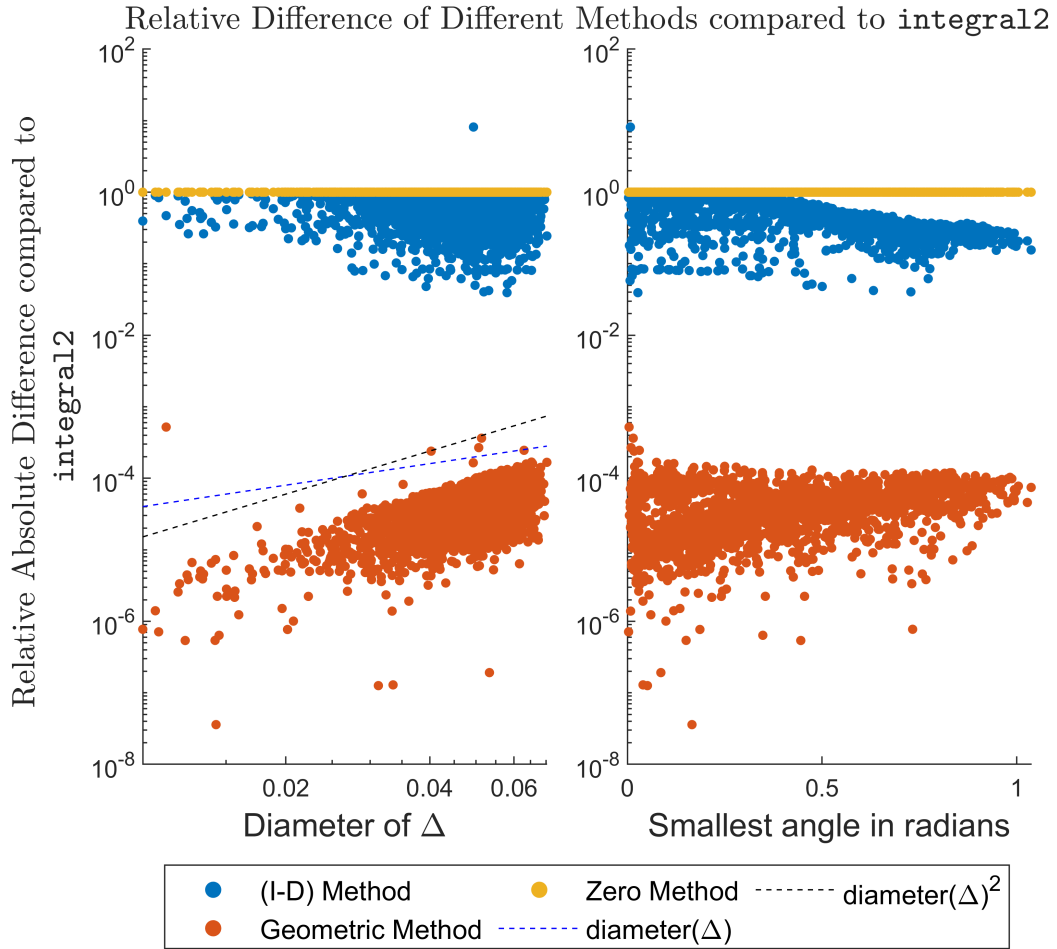


Figure 6: Relative difference of computing the integral Equation 4.1 when \underline{x} is a vertex of Δ on 4000 tests using different methods compared to Matlab’s adaptive method `integral2`. The Zero method means simply setting the integral to equal to zero. In the left subplot, the X-axis is the average norm of the vertices of Δ . The blue dashed line represents a line of slope one, while the black dashed line has slope two. On right subplot, the X-axis is the diameter of Δ . Both subplots show that the Geometric method has a much smaller relative difference compared to the other two methods, though its error depends on the size of Δ . The slope of the line that gives a lower bound for the difference for the Geometric method seems to have slope one. The I-D method on average performs better than the Zero method, but its relative error is high for very small or skewed triangles. Absolute and relative tolerance for `integral2` was set to 10^{-8} .

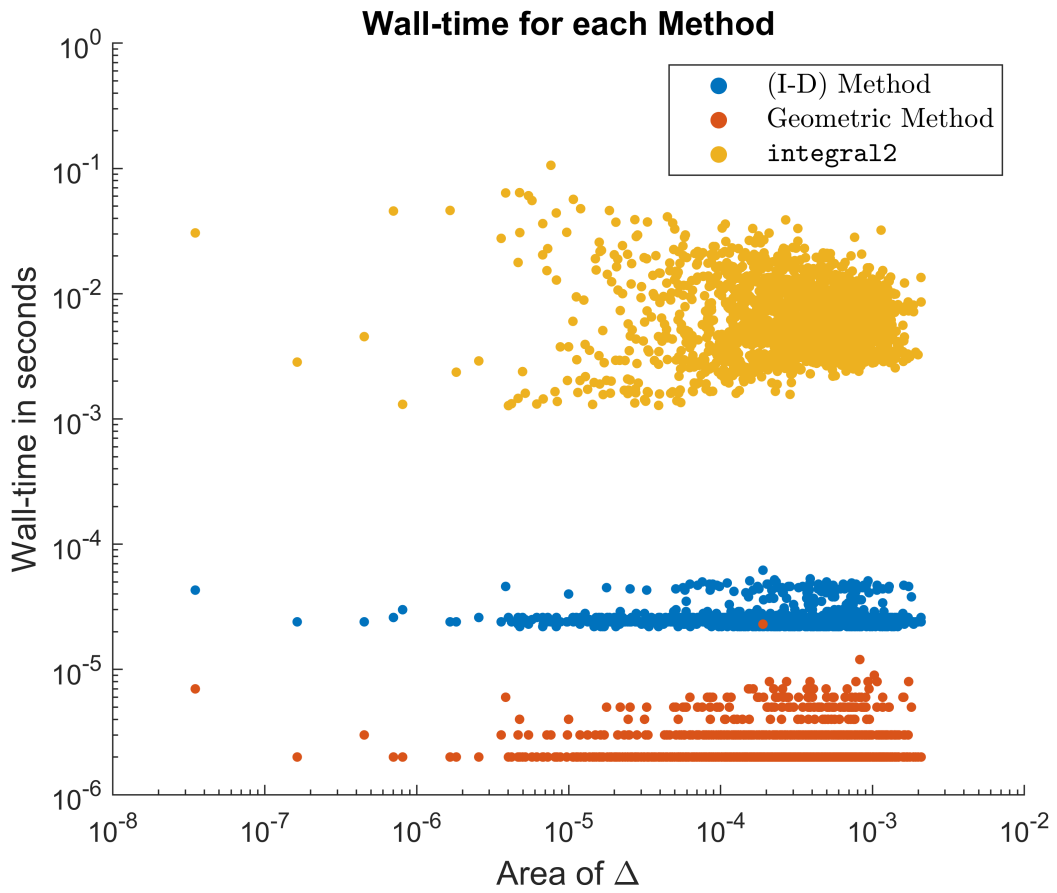


Figure 7: Wall-clock time for the different methods when integrating Equation 4.1 on 4000 tests. The Geometric method is consistently the fastest, with the I-D method around 50 times faster than `integral2`. The Geometric and I-D methods were run on Rust while `integral2` was run in Matlab.

calculating the second fundamental form, either from the function that defines the surface, or by using a finite difference scheme when only a collection of points on the surface is given. Even when the integral is not strongly singular but "near-singular" due to \underline{x} being near Δ , we provide analytic formulas that are just as accurate as adaptive methods when integrating on the simplex Δ while being much faster.

All formulas for the Geometric method for singular integrals and the analytic method for near singular methods are presented for when $p(\underline{y})$ is a degree two polynomial of its components, but can easily be extended to higher polynomials. Analytic formulas for integrating $G(\underline{x}, \underline{y})p(\underline{y})$ are also presented for linear p . As there is no singularity in these integrals, they are accurate no matter where \underline{x} resides.

We believe that with these new formulas, many numerical algorithms of solving PDEs such as BEM [17, 18, 2, 1] can greatly increase their accuracy without the need to heavily refine their discretization of the domain. Especially in the case of BEM, which requires solving a dense linear system, not needing to refine triangular elements allows for a much smaller matrix. This can lead to much faster algorithms and also smaller memory storage due to less elements needed to accurately approximate the domain of integration.

6 Acknowledgments

The authors would like to thank Kirill Serkh for many helpful discussions.

For funding, the work of the authors was supported by the Natural Sciences and Engineering Research Council of Canada (NSERC), grants RGPIN-2020-01113 and RGPIN-2019-06946.

7 Appendix

We list all the formulas needed to evaluate the integrals shown in this paper, and some remarks on their stability.

7.1 Formulas for near singular integrals

Given that

$$\begin{aligned} I_0 &:= \int_{\Delta} \frac{1}{(y_x^2 + y_y^2 + c^2)^{3/2}} dA_{\underline{y}}, & I_x &:= \int_{\Delta} \frac{y_x}{(y_x^2 + y_y^2 + c^2)^{3/2}} dA_{\underline{y}}, \\ I_y &:= \int_{\Delta} \frac{y_y}{(y_x^2 + y_y^2 + c^2)^{3/2}} dA_{\underline{y}}, & I_{x^2} &:= \int_{\Delta} \frac{y_x^2}{(y_x^2 + y_y^2 + c^2)^{3/2}} dA_{\underline{y}}, \\ I_{y^2} &:= \int_{\Delta} \frac{y_y^2}{(y_x^2 + y_y^2 + c^2)^{3/2}} dA_{\underline{y}}, & I_{xy} &:= \int_{\Delta} \frac{y_x y_y}{(y_x^2 + y_y^2 + c^2)^{3/2}} dA_{\underline{y}}. \end{aligned}$$

The integrals that we want to analytically write out in polar coordinates are

$$\int_{r_{\text{start}}}^{r_{\text{end}}} \int_{\theta_{\text{start}}(r)}^{\theta_{\text{end}}(r)} \frac{r^{a+b+1} \cos^a(\theta) \sin^b(\theta)}{(r^2 + c^2)^{3/2}} d\theta dr, \quad (7.1)$$

in which $(a, b) \in \{(0, 0), (1, 0), (0, 1), (2, 0), (0, 2), (1, 1)\}$. The integrals in θ are easy to integrate. After integrating, we substitute $\theta = \phi \pm \arccos(d/r)$ to see what we need to integrate in r .

$$\begin{aligned}
(a, b) = (0, 0) : \quad & \int 1 \, d\theta = \theta = \phi \pm \arccos(d/r), \\
(a, b) = (1, 0) : \quad & \int \cos \theta \, d\theta = \sin \theta = \sin(\phi \pm \arccos(d/r)) \\
& = \frac{d}{r} \sin \phi \pm \frac{\sqrt{r^2 - d^2}}{r} \cos \phi, \\
(a, b) = (0, 1) : \quad & \int \sin \theta \, d\theta = -\cos \theta = -\cos(\phi \pm \arccos(d/r)) \\
& = -\frac{d}{r} \cos \phi \pm \frac{\sqrt{r^2 - d^2}}{r} \sin \phi, \\
(a, b) = (2, 0) : \quad & \int (\cos \theta)^2 \, d\theta = \frac{1}{2}\theta + \frac{1}{2} \cos \theta \sin \theta \\
& = \frac{1}{2}(\phi \pm \arccos(d/r)) \pm \cos(2\phi) \frac{d\sqrt{r^2 - d^2}}{2r^2} + \left(\frac{d^2}{2r^2} - \frac{1}{4}\right) \sin(2\phi), \\
(a, b) = (0, 2) : \quad & \int (\sin \theta)^2 \, d\theta = \frac{1}{2}\theta - \frac{1}{2} \cos \theta \sin \theta \\
& = \frac{1}{2}(\phi \pm \arccos(d/r)) \mp \cos(2\phi) \frac{d\sqrt{r^2 - d^2}}{2r^2} - \left(\frac{d^2}{2r^2} - \frac{1}{4}\right) \sin(2\phi), \\
(a, b) = (1, 1) : \quad & \int \cos \theta \sin \theta \, d\theta = -\frac{1}{2}(\cos \theta)^2 = -\frac{1}{2}(\cos(\phi \pm \arccos(d/r)))^2 \\
& = -\frac{d^2}{2r^2} \cos(2\phi) - \frac{1}{2}(\sin(\phi))^2 \pm \frac{d\sqrt{r^2 - d^2}}{2r^2} \sin(2\phi).
\end{aligned}$$

When you plug these θ integrals into Equation 7.1, there are five integrals in r :

1.

$$\int \frac{r}{(r^2 + c^2)^{3/2}} \, dr = -\frac{1}{\sqrt{r^2 + c^2}},$$

2.

$$\int \frac{r}{(r^2 + c^2)^{3/2}} \arccos \frac{d}{r} \, dr = \begin{cases} -\frac{\arccos \frac{d}{r}}{\sqrt{r^2 + c^2}} + \frac{1}{c} \arctan \left(\frac{c}{d} \sqrt{\frac{r^2 - d^2}{r^2 + c^2}} \right), & d \neq 0, l \neq 0 \\ -\frac{\pi/2}{\sqrt{r^2 + c^2}}, & d = 0 \end{cases},$$

3.

$$\int \frac{r}{(r^2 + c^2)^{3/2}} \sqrt{r^2 - d^2} \, dr = \frac{1}{2} \log \left(2\sqrt{r^2 + c^2} \sqrt{r^2 - d^2} + c^2 - d^2 + 2r^2 \right) - \sqrt{\frac{r^2 - d^2}{r^2 + c^2}},$$

4.

$$\int \frac{r^3}{(r^2 + c^2)^{3/2}} \, dr = \frac{r^2 + 2c^2}{\sqrt{r^2 + c^2}},$$

5.

$$\int \frac{r^3}{(r^2 + c^2)^{3/2}} \arccos \frac{d}{r} dr = \begin{cases} -2c \arctan \left(\frac{c}{d} \sqrt{\frac{r^2 - d^2}{r^2 + c^2}} \right) + \frac{r^2 + 2c^2}{\sqrt{r^2 + c^2}} \arccos \frac{d}{r} - d \operatorname{arctanh} \left(\sqrt{\frac{r^2 - d^2}{r^2 + c^2}} \right), & d \neq 0, r \neq 0 \\ \frac{\pi}{2} \frac{r^2 + 2c^2}{\sqrt{r^2 + c^2}}, & d = 0 \end{cases}.$$

Due to the first integral, we see that c cannot equal to 0 when $r = 0$ (see Equation 7.2). In the case when $c = 0$, the five integrals become

1.

$$\int \frac{1}{r^2} dr = -\frac{1}{r},$$

2.

$$\int \frac{1}{r^2} \arccos \frac{d}{r} dr = \begin{cases} -\frac{\arccos \frac{d}{r}}{r} + \frac{\sqrt{r^2 - d^2}}{rd}, & d \neq 0, l \neq 0 \\ -\frac{\pi/2}{r}, & d = 0 \end{cases},$$

3.

$$\int \frac{1}{r^2} \sqrt{r^2 - d^2} dr = \begin{cases} -\frac{\sqrt{r^2 - d^2}}{r} + \log \left(\frac{\sqrt{r^2 - d^2} + r}{d} \right), & d \neq 0 \\ \log(r), & d = 0 \end{cases},$$

4.

$$\int 1 dr = r,$$

5.

$$\int \arccos \frac{d}{r} dr = \begin{cases} r \arccos \left(\frac{d}{r} \right) - d \log \left(\frac{\sqrt{r^2 - d^2} + r}{d} \right), & d \neq 0, r \neq 0 \\ \frac{\pi}{2} r, & d = 0 \end{cases}.$$

Due to numerical precision, some terms can give NaN values (such as $\operatorname{arctanh} \left(\sqrt{\frac{r^2 - d^2}{r^2 + c^2}} \right)$ when $d^2, c^2 \approx 1e - 16$), so these terms are calculated using the first four terms of their Taylor expansion.

Now we can write out the full formulas for the integrals. For I_0 , we have

$$\begin{aligned} I_0 &= \int_{r_{\text{start}}}^{r_{\text{end}}} \int_{\phi_{\text{start}} + \text{sign}_{\text{start}} \arccos(d_{\text{start}}/r)}^{\phi_{\text{end}} + \text{sign}_{\text{end}} \arccos(d_{\text{end}}/r)} \frac{r}{(r^2 + c^2)^{3/2}} d\theta dr \\ &= (\phi_{\text{end}} - \phi_{\text{start}}) \int_{r_{\text{start}}}^{r_{\text{end}}} \frac{r}{(r^2 + c^2)^{3/2}} dr \\ &\quad + \text{sign}_{\text{end}} \int_{r_{\text{start}}}^{r_{\text{end}}} \frac{r}{(r^2 + c^2)^{3/2}} \arccos \left(\frac{r_{\text{end}}}{r} \right) dr \\ &\quad - \text{sign}_{\text{start}} \int_{r_{\text{start}}}^{r_{\text{end}}} \frac{r}{(r^2 + c^2)^{3/2}} \arccos \left(\frac{d_{\text{start}}}{r} \right) dr. \end{aligned} \tag{7.2}$$

It is important to know that when we have $\phi_{\text{end}} - \phi_{\text{start}}$, we need to check for branch cuts in arctan. These is because ϕ was calculated via arctan, which is multi-valued. If we did not check for branch cuts, we could be potentially integrating $[\theta_{\text{start}}, \theta_{\text{end}} + 2\pi]$ instead of $[\theta_{\text{start}}, \theta_{\text{end}}]$. When checking the branch cut, we just need to check if $\theta_{\text{end}} - \theta_{\text{start}} \in [0, 2\pi]$, **NOT** if $\phi_{\text{end}} - \phi_{\text{start}} \in [0, 2\pi]$. This branch cut problem also shows up in I_{x^2} and I_{y^2} .

For I_x , we have

$$\begin{aligned}
I_x &= \int_{r_{\text{start}}}^{r_{\text{end}}} \int_{\phi_{\text{start}} + \text{sign}_{\text{start}} \arccos(d_{\text{start}}/r)}^{\phi_{\text{end}} + \text{sign}_{\text{end}} \arccos(d_{\text{end}}/r)} \frac{r^2 \cos(\theta)}{(r^2 + c^2)^{3/2}} d\theta dr \\
&= (d_{\text{end}} \sin(\phi_{\text{end}}) - d_{\text{start}} \sin(\phi_{\text{start}})) \int_{r_{\text{start}}}^{r_{\text{end}}} \frac{r}{(r^2 + c^2)^{3/2}} dr \\
&\quad + \text{sign}_{\text{end}} \cos(\phi_{\text{end}}) \int_{r_{\text{start}}}^{r_{\text{end}}} \frac{r \sqrt{r^2 - d_{\text{end}}^2}}{(r^2 + c^2)^{3/2}} dr \\
&\quad - \text{sign}_{\text{start}} \cos(\phi_{\text{start}}) \int_{r_{\text{start}}}^{r_{\text{end}}} \frac{r \sqrt{r^2 - d_{\text{start}}^2}}{(r^2 + c^2)^{3/2}} dr.
\end{aligned} \tag{7.3}$$

For I_y , we have

$$\begin{aligned}
I_y &= \int_{r_{\text{start}}}^{r_{\text{end}}} \int_{\phi_{\text{start}} + \text{sign}_{\text{start}} \arccos(d_{\text{start}}/r)}^{\phi_{\text{end}} + \text{sign}_{\text{end}} \arccos(d_{\text{end}}/r)} \frac{r^2 \sin(\theta)}{(r^2 + c^2)^{3/2}} d\theta dr \\
&= (d_{\text{start}} \cos(\phi_{\text{start}}) - d_{\text{end}} \cos(\phi_{\text{end}})) \int_{r_{\text{start}}}^{r_{\text{end}}} \frac{r}{(r^2 + c^2)^{3/2}} dr \\
&\quad + \text{sign}_{\text{end}} \sin(\phi_{\text{end}}) \int_{r_{\text{start}}}^{r_{\text{end}}} \frac{r \sqrt{r^2 - d_{\text{end}}^2}}{(r^2 + c^2)^{3/2}} dr \\
&\quad - \text{sign}_{\text{start}} \sin(\phi_{\text{start}}) \int_{r_{\text{start}}}^{r_{\text{end}}} \frac{r \sqrt{r^2 - d_{\text{start}}^2}}{(r^2 + c^2)^{3/2}} dr.
\end{aligned} \tag{7.4}$$

For I_{x^2} , we have

$$\begin{aligned}
I_{x^2} &= \int_{r_{\text{start}}}^{r_{\text{end}}} \int_{\phi_{\text{start}} + \text{sign}_{\text{start}} \arccos(d_{\text{start}}/r)}^{\phi_{\text{end}} + \text{sign}_{\text{end}} \arccos(d_{\text{end}}/r)} \frac{r^3 \cos^2(\theta)}{(r^2 + c^2)^{3/2}} d\theta dr \\
&= \frac{1}{2} (\phi_{\text{end}} - \frac{\sin(2\phi_{\text{end}})}{2} - \phi_{\text{start}} + \frac{\sin(2\phi_{\text{start}})}{2}) \int_{r_{\text{start}}}^{r_{\text{end}}} \frac{r^3}{(r^2 + c^2)^{3/2}} dr \\
&\quad + \frac{\text{sign}_{\text{end}}}{2} \int_{r_{\text{start}}}^{r_{\text{end}}} \frac{r^3 \arccos(\frac{d_{\text{end}}}{r})}{(r^2 + c^2)^{3/2}} dr \\
&\quad - \frac{\text{sign}_{\text{start}}}{2} \int_{r_{\text{start}}}^{r_{\text{end}}} \frac{r^3 \arccos(\frac{d_{\text{start}}}{r})}{(r^2 + c^2)^{3/2}} dr \\
&\quad + \frac{1}{2} (d_{\text{end}}^2 \sin(2\phi_{\text{end}}) - d_{\text{start}}^2 \sin(2\phi_{\text{start}})) \int_{r_{\text{start}}}^{r_{\text{end}}} \frac{r}{(r^2 + c^2)^{3/2}} dr \\
&\quad + \frac{1}{2} \text{sign}_{\text{end}} d_{\text{end}} \cos(2\phi_{\text{end}}) \int_{r_{\text{start}}}^{r_{\text{end}}} \frac{r \sqrt{r^2 - d_{\text{end}}^2}}{(r^2 + c^2)^{3/2}} dr \\
&\quad - \frac{1}{2} \text{sign}_{\text{start}} d_{\text{start}} \cos(2\phi_{\text{start}}) \int_{r_{\text{start}}}^{r_{\text{end}}} \frac{r \sqrt{r^2 - d_{\text{start}}^2}}{(r^2 + c^2)^{3/2}} dr.
\end{aligned} \tag{7.5}$$

For I_{y^2} , we have

$$\begin{aligned}
I_{y^2} &= \int_{r_{\text{start}}}^{r_{\text{end}}} \int_{\phi_{\text{start}} + \text{sign}_{\text{start}} \arccos(d_{\text{start}}/r)}^{\phi_{\text{end}} + \text{sign}_{\text{end}} \arccos(d_{\text{end}}/r)} \frac{r^3 \sin^2(\theta)}{(r^2 + c^2)^{3/2}} d\theta dr \\
&= \frac{1}{2} \left(\phi_{\text{end}} + \frac{\sin(2\phi_{\text{end}})}{2} - \phi_{\text{start}} - \frac{\sin(2\phi_{\text{start}})}{2} \right) \int_{r_{\text{start}}}^{r_{\text{end}}} \frac{r^3}{(r^2 + c^2)^{3/2}} dr \\
&\quad + \frac{\text{sign}_{\text{end}}}{2} \int_{r_{\text{start}}}^{r_{\text{end}}} \frac{r^3 \arccos(\frac{d_{\text{end}}}{r})}{(r^2 + c^2)^{3/2}} dr \\
&\quad - \frac{\text{sign}_{\text{start}}}{2} \int_{r_{\text{start}}}^{r_{\text{end}}} \frac{r^3 \arccos(\frac{d_{\text{start}}}{r})}{(r^2 + c^2)^{3/2}} dr \\
&\quad + \frac{1}{2} (-d_{\text{end}}^2 \sin(2\phi_{\text{end}}) + d_{\text{start}}^2 \sin(2\phi_{\text{start}})) \int_{r_{\text{start}}}^{r_{\text{end}}} \frac{r}{(r^2 + c^2)^{3/2}} dr \\
&\quad - \frac{1}{2} \text{sign}_{\text{end}} d_{\text{end}} \cos(2\phi_{\text{end}}) \int_{r_{\text{start}}}^{r_{\text{end}}} \frac{r \sqrt{r^2 - d_{\text{end}}^2}}{(r^2 + c^2)^{3/2}} dr \\
&\quad + \frac{1}{2} \text{sign}_{\text{start}} d_{\text{start}} \cos(2\phi_{\text{start}}) \int_{r_{\text{start}}}^{r_{\text{end}}} \frac{r \sqrt{r^2 - d_{\text{start}}^2}}{(r^2 + c^2)^{3/2}} dr.
\end{aligned} \tag{7.6}$$

For I_{xy} , we have

$$\begin{aligned}
I_{xy} &= \int_{r_{\text{start}}}^{r_{\text{end}}} \int_{\phi_{\text{start}} + \text{sign}_{\text{start}} \arccos(d_{\text{start}}/r)}^{\phi_{\text{end}} + \text{sign}_{\text{end}} \arccos(d_{\text{end}}/r)} \frac{r^3 \sin(\theta) \cos(\theta)}{(r^2 + c^2)^{3/2}} d\theta dr \\
&= \frac{1}{2} (\sin^2(\phi_{\text{start}}) - \sin^2(\phi_{\text{end}})) \int_{r_{\text{start}}}^{r_{\text{end}}} \frac{r^3}{(r^2 + c^2)^{3/2}} dr \\
&\quad + \frac{1}{2} (d_{\text{start}}^2 \cos(2\phi_{\text{start}}) - d_{\text{end}}^2 \cos(2\phi_{\text{end}})) \int_{r_{\text{start}}}^{r_{\text{end}}} \frac{r}{(r^2 + c^2)^{3/2}} dr \\
&\quad + \frac{1}{2} \text{sign}_{\text{end}} \sin(2\phi_{\text{end}}) d_{\text{end}} \int_{r_{\text{start}}}^{r_{\text{end}}} \frac{r \sqrt{r^2 - d_{\text{end}}^2}}{(r^2 + c^2)^{3/2}} dr \\
&\quad - \frac{1}{2} \text{sign}_{\text{start}} \sin(2\phi_{\text{start}}) d_{\text{start}} \int_{r_{\text{start}}}^{r_{\text{end}}} \frac{r \sqrt{r^2 - d_{\text{start}}^2}}{(r^2 + c^2)^{3/2}} dr.
\end{aligned} \tag{7.7}$$

For higher powers, integrating in theta first gives

$$\begin{aligned}
(a, b) = (3, 0) : \quad & \int \cos^3(\theta) d\theta = \sin(\theta) - \frac{1}{3} \sin^3(\theta), \\
(a, b) = (2, 1) : \quad & \int \cos^2(\theta) \sin(\theta) d\theta = -\frac{1}{3} \cos^3(\theta), \\
(a, b) = (1, 2) : \quad & \int \cos(\theta) \sin^2(\theta) d\theta = \frac{1}{3} \sin^3(\theta), \\
(a, b) = (0, 3) : \quad & \int \sin^3(\theta) d\theta = -\cos(\theta) + \frac{1}{3} \cos^3(\theta).
\end{aligned}$$

Plugging in $\theta = \phi \pm \arccos(d/r)$, we get for $(a, b) = (3, 0)$

$$(a, b) = (3, 0) : \left(\sin(\theta) \frac{d}{r} \pm \cos(\phi) \frac{\sqrt{r^2 - d^2}}{r} \right) - \frac{1}{3} \left[\sin^3(\phi) \frac{d^3}{r^3} \pm 3 \sin^2(\phi) \cos(\phi) \frac{d^2 \sqrt{r^2 - d^2}}{r^3} + 3 \sin(\phi) \cos^2(\phi) \frac{d(r^2 - d^2)}{r^3} \pm \cos^3(\phi) \frac{(r^2 - d^2)^{3/2}}{r^3} \right].$$

For $(a, b) = (0, 3)$, we have

$$(a, b) = (0, 3) : - \left(\cos(\theta) \frac{d}{r} \mp \sin(\phi) \frac{\sqrt{r^2 - d^2}}{r} \right) + \frac{1}{3} \left[\cos^3(\phi) \frac{d^3}{r^3} \mp 3 \cos^2(\phi) \sin(\phi) \frac{d^2 \sqrt{r^2 - d^2}}{r^3} + 3 \cos(\phi) \sin^2(\phi) \frac{d(r^2 - d^2)}{r^3} \mp \sin^3(\phi) \frac{(r^2 - d^2)^{3/2}}{r^3} \right].$$

Integrating in r , we have the extra integral is

$$\int \frac{r(r^2 - d^2)^{3/2}}{(r^2 + c^2)^{3/2}} dr = \sqrt{\frac{r^2 - d^2}{r^2 + c^2}} \frac{r^2 + 2d^2 + 3c^2}{2} - \frac{3(c^2 + d^2) \log(\sqrt{r^2 + c^2} + \sqrt{r^2 - d^2})}{2}.$$

When $c = 0$, we have that the integral becomes

$$\int \frac{(r^2 - d^2)^{3/2}}{r^2} dr = \left(\frac{d^2}{r} + \frac{r}{2} \right) \sqrt{r^2 - d^2} - \frac{3d^2}{2} \log(r + \sqrt{r^2 - d^2}).$$

These equations can then be used to get the integrals for $(a, b) = (2, 1)$ or $(a, b) = (1, 2)$.

7.2 Formulas for the Geometric method

Recall that in the Geometric method, the integrals are of the form

$$\int_0^{\theta_{\text{end}}} (\cos(\theta))^a (\sin(\theta))^b \int_0^{r(\theta)} r^{a+b+1-3} dr d\theta. \quad (7.8)$$

This simple formula is only because we can fix one edge to be the X -axis, so that the integral in θ starts at zero. The integrals in r are trivial as $a + b + 1 - 3 \geq 0$, so we get

$$\int_0^{\theta_{\text{end}}} (\cos(\theta))^a (\sin(\theta))^b \frac{1}{a + b - 1} \left(\frac{|pV_2| \sin(\theta_2)}{\sin(\theta + \theta_2)} \right)^{a+b-1} d\theta. \quad (7.9)$$

We shall only consider the cases in which $(a, b) \in \{(1, 1), (2, 0), (0, 2), (2, 1), (1, 2), (3, 0), (0, 3)\}$. These correspond to when we approximate p using linear functions, but it is not difficult to write similar formulas for higher powers.

For notation, we write

$$\begin{aligned}\tilde{I}_{x^2} &= \int_0^{\theta_{\text{end}}} \frac{\cos^2(\theta)}{\sin(\theta + \theta_2)} d\theta, & \tilde{I}_{y^2} &= \int_0^{\theta_{\text{end}}} \frac{\sin^2(\theta)}{\sin(\theta + \theta_2)} d\theta, \\ \tilde{I}_{x^2y} &= \int_0^{\theta_{\text{end}}} \frac{\cos^2(\theta) \sin(\theta)}{\sin^2(\theta + \theta_2)} d\theta, & \tilde{I}_{xy^2} &= \int_0^{\theta_{\text{end}}} \frac{\cos(\theta) \sin^2(\theta)}{\sin^2(\theta + \theta_2)} d\theta, \\ \tilde{I}_{x^3} &= \int_0^{\theta_{\text{end}}} \frac{\cos^3(\theta)}{\sin^2(\theta + \theta_2)} d\theta, & \tilde{I}_{y^3} &= \int_0^{\theta_{\text{end}}} \frac{\sin^3(\theta)}{\sin^2(\theta + \theta_2)} d\theta.\end{aligned}$$

The integrals are as follows.

$$\begin{aligned}
(a, b) = (1, 1) &: \int \frac{\cos(\theta) \sin(\theta)}{\sin(\theta + \theta_2)} d\theta \\
&= \sin(\theta - \theta_2) - \frac{\sin(2\theta_2)}{2} \log \left(\tan\left(\frac{\theta + \theta_2}{2}\right) \right), \\
(a, b) = (2, 0) &: \int \frac{\cos^2(\theta)}{\sin(\theta + \theta_2)} d\theta \\
&= \cos(\theta - \theta_2) + \cos^2(\theta_2) \log \left(\tan \left(\frac{\theta + \theta_2}{2} \right) \right), \\
(a, b) = (0, 2) &: \int \frac{\sin^2(\theta)}{\sin(\theta + \theta_2)} d\theta \\
&= -\cos(\theta - \theta_2) + \sin^2(\theta_2) \log \left(\tan \left(\frac{\theta + \theta_2}{2} \right) \right), \\
(a, b) = (2, 1) &: \int \frac{\cos^2(\theta) \sin(\theta)}{\sin^2(\theta + \theta_2)} d\theta \\
&= \frac{1}{4} \left(-2(\cos(\theta_2) + 3 \cos(3\theta_2)) \operatorname{arctanh} \left(\cos(\theta_2) - \sin(\theta_2) \tan \left(\frac{\theta}{2} \right) \right) \right. \\
&\quad \left. + \csc(\theta + \theta_2) (2 \sin(2\theta - \theta_2) + \sin(\theta_2) + 3 \sin(3\theta_2)) \right), \\
(a, b) = (1, 2) &: \int \frac{\cos(\theta) \sin^2(\theta)}{\sin^2(\theta + \theta_2)} d\theta \\
&= \frac{1}{4} \left(-2(\sin(\theta_2) - 3 \sin(3\theta_2)) \operatorname{arctanh} \left(\cos(\theta_2) - \sin(\theta_2) \tan \left(\frac{\theta}{2} \right) \right) \right. \\
&\quad \left. - \csc(\theta + \theta_2) (2 \cos(2\theta - \theta_2) + \cos(\theta_2) - 3 \cos(3\theta_2)) \right), \\
(a, b) = (3, 0) &: \int \frac{\cos^3(\theta)}{\sin^2(\theta + \theta_2)} d\theta \\
&= -\cos(\theta - 2\theta_2) - 6 \cos(\theta_2) \sin^2(\theta_2) \operatorname{arctanh} \left(\cos(\theta_2) - \sin(\theta_2) \tan \left(\frac{\theta}{2} \right) \right) \\
&\quad + \sin^3(\theta_2) \csc(\theta + \theta_2), \\
(a, b) = (0, 3) &: \int \frac{\sin^3(\theta)}{\sin^2(\theta + \theta_2)} d\theta \\
&= -\sin(\theta - 2\theta_2) - 6 \cos^2(\theta_2) \sin(\theta_2) \operatorname{arctanh} \left(\cos(\theta_2) - \sin(\theta_2) \tan \left(\frac{\theta}{2} \right) \right) \\
&\quad - \cos^3(\theta_2) \csc(\theta + \theta_2).
\end{aligned}$$

7.3 Formulas for Green's function

Though most of the paper discusses integrating $K(\underline{x}, \underline{y})p(\underline{y})$, we also provide analytic equations for integrating $G(\underline{x}, \underline{y})p(\underline{y})$ where G is defined from Equation 1.3 and $p(\underline{y})$ is a linear function. Given

$$\begin{aligned} J_0 &:= \int_{\Delta} \frac{1}{(y_x^2 + y_y^2 + c^2)^{1/2}} dA_{\underline{y}}, \\ J_x &:= \int_{\Delta} \frac{y_x}{(y_x^2 + y_y^2 + c^2)^{1/2}} dA_{\underline{y}}, \\ J_y &:= \int_{\Delta} \frac{y_y}{(y_x^2 + y_y^2 + c^2)^{1/2}} dA_{\underline{y}}. \end{aligned}$$

The desired integral is

$$J = -\frac{1}{4\pi} \sum_{i=1}^3 \gamma(V_i) [l_{i,0}J_0 + l_{i,x}J_x + l_{i,y}J_y].$$

The integrals are of the form

$$\int_{r_{\text{start}}}^{r_l} \int_{\theta_{\text{start}}}^{\theta_{\text{end}}} \frac{r^{a+b+1} (\cos(\theta))^a (\sin(\theta))^b}{(r^2 + c^2)^{1/2}} \quad (7.10)$$

for $(a, b) = \{(0, 0), (0, 1), (1, 0)\}$. The integrals in θ are

$$\begin{aligned} (a, b) = (0, 0) : & \quad \int 1 d\theta = \theta = \phi \pm \arccos\left(\frac{d}{r}\right), \\ (a, b) = (1, 0) : & \quad \int \cos(\theta) d\theta = \sin(\theta) = \sin\left(\phi \pm \arccos\left(\frac{d}{r}\right)\right) \\ & \quad = \frac{d}{r} \sin(\phi) \pm \frac{\sqrt{r^2 - d^2}}{r} \cos(\phi), \\ (a, b) = (0, 1) : & \quad \int \sin(\theta) d\theta = -\cos(\theta) = -\cos\left(\phi \pm \arccos\left(\frac{d}{r}\right)\right) \\ & \quad = -\frac{d}{r} \cos(\phi) \pm \frac{\sqrt{r^2 - d^2}}{r} \sin(\phi). \end{aligned}$$

The integrals in r are calculated to be

1.

$$\int \frac{r}{(r^2 + c^2)^{1/2}} dr = \sqrt{r^2 + c^2},$$

2.

$$\int \frac{r \arccos\left(\frac{d}{r}\right)}{(r^2 + c^2)^{1/2}} dr = \begin{cases} \sqrt{r^2 + c^2} \arccos\left(\frac{d}{r}\right) - c \arcsin\left(\frac{c\sqrt{r^2 - d^2}}{\sqrt{c^2 + d^2}}\right) - d \operatorname{arctanh}\left(\sqrt{\frac{r^2 - d^2}{r^2 + c^2}}\right) & d, r \neq 0, \\ \frac{\pi}{2} \sqrt{r^2 + c^2} & d = 0 \end{cases},$$

3.

$$\int \frac{r\sqrt{r^2-d^2}}{(r^2+c^2)^{1/2}} dr = \frac{1}{2} \left(\sqrt{r^2+c^2}\sqrt{r^2-d^2} + (c^2+d^2) \log(\sqrt{r^2+c^2} - \sqrt{r^2-d^2}) \right).$$

Note here that the sign of c does not matter on both sides of the equations. In the right hand side of the second integral, arcsin is a odd function, so the sign of the c inside and in front of arcsin cancel each other out. Unlike the Neumann problem, c can equal to 0 on the left hand side even if $r = 0$. When $c = 0$, the integrals are

1.

$$\int \frac{r}{(r^2)^{1/2}} dr = r,$$

2.

$$\int \frac{r \arccos(\frac{d}{r})}{(r^2)^{1/2}} dr = \begin{cases} r \arccos(\frac{d}{r}) + \frac{d}{2} \log\left(-\frac{\sqrt{r^2-d^2}-r}{\sqrt{r^2-d^2}+r}\right) & d, r \neq 0 \\ \frac{\pi}{2}r & d = 0 \end{cases},$$

3.

$$\int \frac{r\sqrt{r^2-d^2}}{(r^2)^{1/2}} dr = \begin{cases} \frac{1}{2} (r\sqrt{r^2-d^2} + d^2 \log(r - \sqrt{r^2-d^2})) & d, r \neq 0 \\ \frac{1}{2}r^2 & d = 0 \end{cases}.$$

Hence,

$$\begin{aligned} J_0 &= \int_{r_{\text{start}}}^{r_{\text{end}}} \int_{\phi_{\text{start}} + \text{sign}_{\text{start}} \arccos(d_{\text{start}}/r)}^{\phi_{\text{end}} + \text{sign}_{\text{end}} \arccos(d_{\text{end}}/r)} \frac{r}{(r^2+c^2)^{1/2}} d\theta dr \\ &= (\phi_{\text{end}} - \phi_{\text{start}}) \int_{r_{\text{start}}}^{r_{\text{end}}} \frac{r}{(r^2+c^2)^{1/2}} dr \\ &+ \text{sign}_{\text{end}} \int_{r_{\text{start}}}^{r_{\text{end}}} \frac{r}{(r^2+c^2)^{1/2}} \arccos\left(\frac{d_{\text{end}}}{r}\right) dr \\ &- \text{sign}_{\text{start}} \int_{r_{\text{start}}}^{r_{\text{end}}} \frac{r}{(r^2+c^2)^{1/2}} \arccos\left(\frac{d_{\text{start}}}{r}\right) dr. \end{aligned}$$

$$\begin{aligned} J_x &= \int_{r_{\text{start}}}^{r_{\text{end}}} \int_{\phi_{\text{start}} + \text{sign}_{\text{start}} \arccos(d_{\text{start}}/r)}^{\phi_{\text{end}} + \text{sign}_{\text{end}} \arccos(d_{\text{end}}/r)} \frac{r^2 \cos(\theta)}{(r^2+c^2)^{1/2}} d\theta dr \\ &= (d_{\text{end}} \sin(\phi_{\text{end}}) - d_{\text{start}} \sin(\phi_{\text{start}})) \int_{r_{\text{start}}}^{r_{\text{end}}} \frac{r}{(r^2+c^2)^{1/2}} dr \\ &+ \text{sign}_{\text{end}} \cos(\phi_{\text{end}}) \int_{r_{\text{start}}}^{r_{\text{end}}} \frac{r\sqrt{r^2-d_{\text{end}}^2}}{(r^2+c^2)^{1/2}} dr \\ &- \text{sign}_{\text{start}} \cos(\phi_{\text{start}}) \int_{r_{\text{start}}}^{r_{\text{end}}} \frac{r\sqrt{r^2-d_{\text{start}}^2}}{(r^2+c^2)^{1/2}} dr. \end{aligned}$$

$$\begin{aligned}
J_y &= \int_{r_{\text{start}}}^{r_{\text{end}}} \int_{\phi_{\text{start}} + \text{sign}_{\text{start}} \arccos(d_{\text{start}}/r)}^{\phi_{\text{end}} + \text{sign}_{\text{end}} \arccos(d_{\text{end}}/r)} \frac{r^2 \sin(\theta)}{(r^2 + c^2)^{1/2}} d\theta dr \\
&= -(d_{\text{end}} \cos(\phi_{\text{end}}) - d_{\text{start}} \cos(\phi_{\text{start}})) \int_{r_{\text{start}}}^{r_{\text{end}}} \frac{r}{(r^2 + c^2)^{1/2}} dr \\
&\quad + \text{sign}_{\text{end}} \sin(\phi_{\text{end}}) \int_{r_{\text{start}}}^{r_{\text{end}}} \frac{r \sqrt{r^2 - d_{\text{end}}^2}}{(r^2 + c^2)^{1/2}} dr \\
&\quad - \text{sign}_{\text{start}} \sin(\phi_{\text{start}}) \int_{r_{\text{start}}}^{r_{\text{end}}} \frac{r \sqrt{r^2 - d_{\text{start}}^2}}{(r^2 + c^2)^{1/2}} dr.
\end{aligned}$$

Just like before, we need to be careful of the branch cut problem in J_x . As all integrals are finite even when $c = 0$, \underline{x} can be any arbitrary point in \mathbb{R}^3 .

References

- [1] Kendall E Atkinson. *The numerical solution of integral equations of the second kind*. Vol. 4. Cambridge university press, 1997.
- [2] Sebastian Bohm and Erich Runge. “Efficient analytical evaluation of the singular BEM integrals for the three-dimensional Laplace and Stokes equations over polygonal elements”. In: *Engineering Analysis with Boundary Elements* 161 (2024), pp. 70–77.
- [3] W Cai, Yijun Yu, and XC Yuan. “Singularity treatment and high-order RWG basis functions for integral equations of electromagnetic scattering”. In: *International journal for numerical methods in engineering* 53.1 (2002), pp. 31–47.
- [4] Michael J Carley. “Analytical formulae for potential integrals on triangles”. In: *Journal of Applied Mechanics* 80.4 (2013), p. 041008.
- [5] Boris Delaunay. “Sur la sphère vide”. In: *Bulletin of the Academy of Sciences of the USSR, Class of Mathematical and Natural Sciences* 6 (1934), pp. 793–800.
- [6] Manfredo P Do Carmo. *Differential geometry of curves and surfaces: revised and updated second edition*. Courier Dover Publications, 2016.
- [7] Michael G Duffy. “Quadrature over a pyramid or cube of integrands with a singularity at a vertex”. In: *SIAM journal on Numerical Analysis* 19.6 (1982), pp. 1260–1262.
- [8] Roberto D Graglia. “On the numerical integration of the linear shape functions times the 3-D Green’s function or its gradient on a plane triangle”. In: *IEEE transactions on antennas and propagation* 41.10 (1993), pp. 1448–1455.
- [9] Boyce E Griffith and Charles S Peskin. “Electrophysiology”. In: *Communications on Pure and Applied Mathematics* 66.12 (2013), pp. 1837–1913.
- [10] George C Hsiao and Wolfgang L Wendland. *Boundary integral equations*. Springer, 2008.
- [11] Seppo Järvenpää, Matti Taskinen, and Pasi Ylä-Oijala. “Singularity extraction technique for integral equation methods with higher order basis functions on plane triangles and tetrahedra”. In: *International journal for numerical methods in engineering* 58.8 (2003), pp. 1149–1165.
- [12] Tadeusz Liszka and Janusz Orkisz. “The finite difference method at arbitrary irregular grids and its application in applied mechanics”. In: *Computers & Structures* 11.1-2 (1980), pp. 83–95.

- [13] V Mantič. “On computing boundary limiting values of boundary integrals with strongly singular and hypersingular kernels in 3D BEM for elastostatics”. In: *Engineering Analysis with Boundary Elements* 13.2 (1994), pp. 115–134.
- [14] SE Mousavi and N Sukumar. “Generalized Duffy transformation for integrating vertex singularities”. In: *Computational Mechanics* 45 (2010), pp. 127–140.
- [15] Ephraim E Okon and Roger F Harrington. “The potential integral for a linear distribution over a triangular domain”. In: *International Journal for Numerical Methods in Engineering* 18.12 (1982), pp. 1821–1828.
- [16] Per-Olof Persson and Gilbert Strang. “A simple mesh generator in MATLAB”. In: *SIAM review* 46.2 (2004), pp. 329–345.
- [17] Matjaž Ramšak and Leopold Škerget. “3D multidomain BEM for solving the Laplace equation”. In: *Engineering analysis with boundary elements* 31.6 (2007), pp. 528–538.
- [18] Qinlong Ren and Cho Lik Chan. “Analytical evaluation of the BEM singular integrals for 3D Laplace and Stokes flow equations using coordinate transformation”. In: *Engineering Analysis with Boundary Elements* 53 (2015), pp. 1–8.
- [19] V Sladek, J Sladek, and M Tanaka. “Optimal transformations of the integration variables in computation of singular integrals in BEM”. In: *International journal for numerical methods in engineering* 47.7 (2000), pp. 1263–1283.
- [20] Victor A Toponogov. *Differential geometry of curves and surfaces*. Springer, 2006.